

# Label Words are Anchors: An Information Flow Perspective for Understanding In-Context Learning

Lean Wang<sup>†</sup>, Lei Li<sup>†</sup>, Damai Dai<sup>†</sup>, Deli Chen<sup>§</sup>,  
Hao Zhou<sup>§</sup>, Fandong Meng<sup>§</sup>, Jie Zhou<sup>§</sup>, Xu Sun<sup>†</sup>

<sup>†</sup>National Key Laboratory for Multimedia Information Processing,  
School of Computer Science, Peking University

<sup>§</sup>Pattern Recognition Center, WeChat AI, Tencent Inc., China  
{lean, daidama, xusun}@pku.edu.cn nlp.lilei@gmail.com  
{delichen, tuxzhou, fandongmeng, withtomzhou}@tencent.com

## Abstract

In-context learning (ICL) emerges as a promising capability of large language models (LLMs) by providing them with demonstration examples to perform diverse tasks. However, the underlying mechanism of how LLMs learn from the provided context remains under-explored. In this paper, we investigate the working mechanism of ICL through an information flow lens. Our findings reveal that label words in the demonstration examples function as anchors: (1) semantic information aggregates into label word representations during the shallow computation layers' processing; (2) the consolidated information in label words serves as a reference for LLMs' final predictions. Based on these insights, we introduce an anchor re-weighting method to improve ICL performance, a demonstration compression technique to expedite inference, and an analysis framework for diagnosing ICL errors in GPT2-XL. The promising applications of our findings again validate the uncovered ICL working mechanism and pave the way for future studies.

## 1 Introduction

In-context Learning (ICL) has emerged as a powerful capability alongside the development of scaled-up large language models (LLMs) (Brown et al., 2020). By instructing LLMs using few-shot demonstration examples, ICL enables them to perform a wide range of tasks, such as text classification (Min et al., 2022a) and mathematical reasoning (Wei et al., 2022). Since ICL does not require updates to millions or trillions of model parameters and relies on human-understandable natural language instructions (Dong et al., 2023), it has become a promising approach for harnessing the full potentiality of LLMs. Despite its significance, the inner working mechanism of ICL remains an open question, garnering considerable interest from research communities (Xie et al., 2022; von Oswald et al., 2022; Dai et al., 2022; Olsson et al., 2022).



Figure 1: Saliency visualization results of shallow and deep layers of a GPT model. Here, the depth of the line from the right word to the left word reflects the importance of the information flow in ICL.

In this paper, we find that the label words serve as anchors that aggregate and distribute information in ICL. Specifically, we first visualize the attention interactive pattern between tokens with a GPT model (Brown et al., 2020) on sentiment analysis. As shown in Figure 1, we have an intuitive observation that as the layer goes deeper, the label words in the demonstration will become more dominant for the prediction. To draw a clearer picture of this phenomenon, we compute two metrics based on saliency scores to portray the information flow in ICL and further propose the following hypothesis:

### Information Flow with Labels as Anchors

$\mathcal{H}_1$ : In shallow layers, label words gather the information of demonstrations to form semantic representations for deeper layers.

$\mathcal{H}_2$ : In deep layers, the model extracts the information from label words to form the final prediction.

We design two experiments to validate the hypothesis using GPT2-XL (Radford et al., 2019) and

GPT-J (Wang and Komatsuzaki, 2021) on various text classification benchmarks. (1) By isolating the label words in certain layers to block the information aggregation path to the label words, we find that such isolation in shallow layers significantly impairs model performance. This indicates that label words indeed collect useful semantics during the forward propagation in shallow layers. (2) We examine the correlation between the attention distributions on the label words of the target position and the final prediction results. The results show that the prediction positively correlates with the attention weights on label words, i.e., the probability of a candidate is higher with more attention weights on the specific label. In summary, these experimental findings suggest that our hypothesis holds well with large language models on real-world datasets.

Drawing on insights from the information flow perspective, we explore three approaches to enhance ICL’s effectiveness, efficiency, and interpretability. (1) We introduce an anchor re-weighting method utilizing a learnable vector to adaptively adjust the significance of various label words in demonstration examples, achieving a 16.7 average accuracy improvement over vanilla ICL baselines. (2) To expedite ICL inference, we compress its input into pre-computed anchor representations, as model predictions primarily rely on label word activations. Experiments demonstrate that the inference can be accelerated  $1.8 \times$  with negligible performance degradation. (3) We present an error analysis example using ICL on GPT2-XL, revealing that the label confusion matrix closely mirrors the distance distribution of anchor key vectors, suggesting errors may arise from indistinguishable anchor representations. These promising applications further validate our hypothesis and shed light on future ICL studies for better transparency of LLMs.

## 2 Label Words are Anchors

In this section, we first confirm our intuitive findings with two metrics based on saliency scores in § 2.1. Based on the quantitative results, we further propose the hypothesis to interpret the working mechanism of ICL:  $\mathcal{H}_1$ : In shallow layers, label words aggregate information from demonstration examples to form semantic representations for later computations.  $\mathcal{H}_2$ : In deep layers, the model makes predictions by extracting information from label words. We validate these two hypothesis in § 2.2 and § 2.3, respectively.

### 2.1 Hypothesis Motivated by Saliency Scores

In this part, we aim to visualize the attention interactive pattern between tokens for GPT2-XL, and find patterns behind such interaction. We utilize a common interpretation tool, saliency technique (Simonyan et al., 2013), to reveal the important token interactions. Following common practice, we use the Taylor expansion (Michel et al., 2019) to calculate the saliency score for each element of the attention matrix:

$$I_l = \sum_h \left| A_{h,l}^\top \frac{\partial \mathcal{L}(x)}{\partial A_{h,l}} \right| \quad (1)$$

Here,  $A_{h,l}$  is the value of the attention matrix of the  $h$ -th attention head in the  $l$ -th layer,  $x$  is the input, and  $\mathcal{L}(x)$  is the loss function of the task, e.g., the cross-entropy objective for a classification problem. We average all attention heads to obtain the saliency matrix  $I_l$  for the  $l$ -th layer.  $I_l(i, j)$  represents the importance of the information flow from the  $j$ -th word to the  $i$ -th word for ICL. By observing  $I_l$ , we can get an intuitive impression that as the layer goes deeper, demonstration label words will become more dominant for the prediction, as depicted in Figure 1.

To draw a clearer picture of this phenomenon, we propose the following quantitative metrics base on  $I_l$ . Let the positions of the label words in the input  $x$  be  $p_1, \dots, p_C$ , the target position be  $q$ , and the saliency matrix of the  $l$ -th layer be  $I_l$ . Then, we define three quantitative metrics:

**$S_{wp}$ , the average importance of the information flow from other words to label words:**

$$S_{wp} = \frac{\sum_{(i,j) \in C_{wp}} I_l(i, j)}{|C_{wp}|}, \quad (2)$$

$$C_{wp} = \{(p_k, j) : k \in [1, C], j < p_k\}.$$

**$S_{pq}$ , the average importance of the information flow from label words to the target position:**

$$S_{pq} = \frac{\sum_{(i,j) \in C_{pq}} I_l(i, j)}{|C_{pq}|}, \quad (3)$$

$$C_{pq} = \{(p_k, q) : k \in [1, C]\}.$$

**$S_{ww}$ , the average importance of the information flow between any words (excluding  $S_{wp}$  and  $S_{pq}$ ):**

$$S_{ww} = \frac{\sum_{(i,j) \in C_{ww}} I_l(i, j)}{|C_{ww}|}, \quad (4)$$

$$C_{ww} = \{(i, j) : j < i\} \\ - C_{wp} - C_{pq}.$$

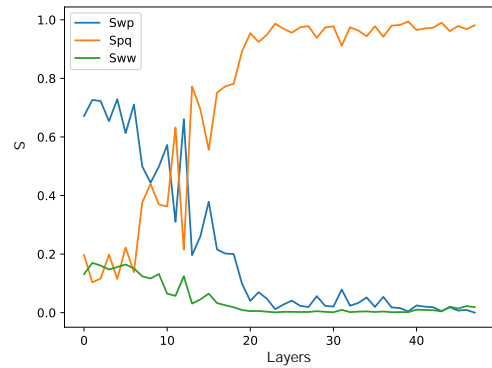
**Experimental Settings** We choose GPT2-XL from the GPT series (Radford et al., 2019) as the main model to be examined, due to its moderate model size (of 1.5B parameters) that is suitable for our hardware resource and its decent ICL performance (Dai et al., 2022). For datasets, we use a sentiment analysis task, Stanford Sentiment Treebank Binary (SST-2) (Socher et al., 2013), a question type classification task, Text REtrieval Conference Question Classification (TREC) (Li and Roth, 2002; Hovy et al., 2001), a topic classification task, AG’s news topic classification dataset (AG-News) (Zhang et al., 2015), an emotion classification task, EmoContext (EmoC) (Chatterjee et al., 2019). The templates used for constructing demonstrations of these datasets can be found in Appendix A. We extracted 1000 examples from the test set for evaluation. For ease of analysis, we sample one example for each class from the training set to form the demonstration, and the demonstration order follows a random order. All results are averaged over five random seeds.

**Results and Analysis** The results are shown in Figure 2. It can be seen that (1) in the shallow layers,  $S_{pq}$ , the importance of the information flow from label words to targeted positions is low, while  $S_{wp}$ , the information flow from other words to label words is high; (2) in the deep layers,  $S_{pq}$ , the importance of information flow from label words to the targeted position become the dominant one. Meanwhile,  $S_{pq}$  and  $S_{wp}$  are usually more than  $S_{ww}$ , indicating that the interactions involving label words are more important than others.

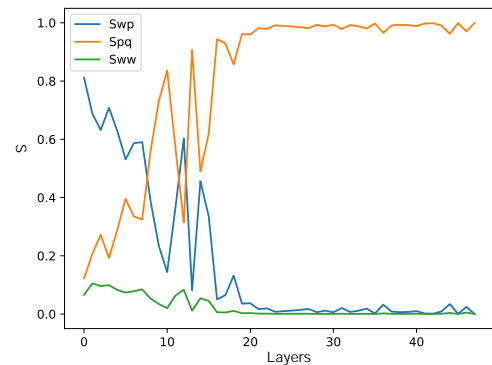
**Proposed Hypothesis** Based on this, we propose the hypothesis that label words function as anchors in the ICL information flow. In shallow layers, label words gather information from demonstration examples to form semantic representations for deeper layers, while in deep layers, the model extracts the information from label words to form the final prediction.

## 2.2 Shallow Layers: Information Aggregation

In this part, we validate the first part of our hypothesis. We hypothesize that the aggregation of information in in-context learning relies on the flow of information from demonstration tokens to label tokens, which is facilitated by the attention mechanism in transformers. By manipulating attention to block this information flow and examining the changes in model behavior, we can validate



(a) Results on the SST-2 dataset



(b) Results on the AGNews dataset

Figure 2: Relationship between the relative sizes of  $S_{wp}$ ,  $S_{pq}$ , and  $S_{ww}$  and the number of layers. (We normalized  $(S_{wp}, S_{pq}, S_{ww})$ ) Results of TREC and EmoC can be seen in Appendix D. Initially,  $S_{wp}$  occupies a significant proportion, but it gradually decays over the layers, while  $S_{pq}$  becomes the dominant one.

whether the information aggregation process exists and how much it contributes to the final predictions.

**Experimental Settings** We maintain the same sample size of 1000 inputs from the test set as Section 2.1. We use the same demonstration for a single random seed. To further validate our findings on larger models, we incorporate GPT-J (6B) (Wang and Komatsuzaki, 2021) in our experiments, which surpasses GPT2-XL in terms of model size and capacity.

**Implementation Details** To achieve the intervention on the information flow on the label words, we isolate label words in certain layers, by disabling the attention from the label words attending to the demonstrations. Specifically, we set  $A_{l,h}(p, i) (i < p)$  in the attention matrix  $A_{l,h}$  of each attention head in the  $l$ -th layer to 0, where  $p$  is

Isolation Layer	Label Loyalty	Word Loyalty
GPT2-XL No isolation	100.00	100.00
First 5 layers	44.03	6.30
Last 5 layers	99.61	99.52
GPT-J No isolation	100.00	100.00
First 5 layers	62.13	53.77
Last 5 layers	99.01	97.76

Table 1: Effects of isolating label words, results are averaged across the SST-2, TREC, AGNews, and EmoC datasets (percentage). Isolating the first 5 layers significantly reduces the loyalty.

the position of the label word, and  $i$  is the position of the word before the label word. Therefore, label words in the  $l$ -th layer cannot receive the information from previous demonstration examples via the attention mechanism.

**Metrics** To measure the effects of blocking the information flow from demonstration tokens to label tokens, we use the following metrics to examine the changes in the model predictions: **(1) Label Loyalty:** which measures the consistency between the outputs labels with and without isolation. Higher label loyalty indicates that the model predictions are less affected by the isolation. **(2) Word Loyalty:** which probes more fine-grained changes on the model predictions. Specifically, we adopt the Jaccard similarity between the top-5 potential words drawn from the original vocabulary distributions and that after isolation. This metric could capture subtle changes in the output distributions, where higher word loyalty indicates better consistency between the language model outputs. We refer readers to Appendix B for a detailed discussion.

**Results and Analysis** We isolate the label words in the first 5 layers to examine the existence and effect of information aggregation. We also isolate the label words in the last 5 layers for comparison. As shown in Table 1, isolating label words in the first 5 layers can cause serious interference to the model’s task completion, while the impact of the last 5 layers is small. This verifies the existence of information aggregation in shallow layers, and demonstrates its significance in ICL. We also explore the isolation effects by varying the number of labels disabled in Appendix C and observe a similar trend.

## 2.3 Deep Layers: Information Extraction

We further validate the second part of our hypothesis, i.e., the model extracts the information from label words to form the final prediction. We examine the correlation between the attention distributions on the label words of the target position and the model’s final prediction.

We use the same dataset and model setup as in § 2.2.

### 2.3.1 Experiments

Suppose the positions of the label words in the input  $x$  are  $p_1, \dots, p_C$ , the targeted position is  $q$ , and the sum of the attention matrices of each attention head at the  $l$ -th layer is  $A_l$ . We postulate that there’s a strong correlation between the attention distributions on the label words of the target position ( $A_l(q, p_1), \dots, A_l(q, p_C)$ ) and the model’s final prediction. We use the AUC-ROC score to quantify this correlation, which we denote as  $\text{AUCROC}_l$ .

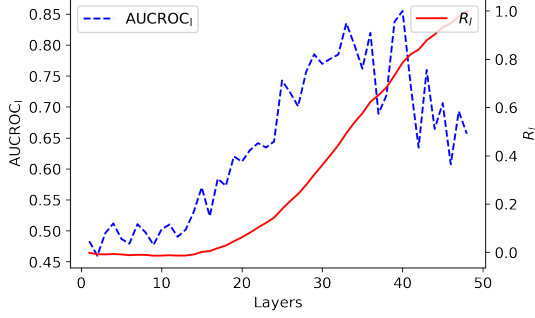
We use AUC-ROC for two reasons: (1) Considering the attention mechanism, the attention values are used to weigh the key vectors. The size of the attention cannot fully reflect the importance of the corresponding word; it must be combined with factors such as the norm of the key vector (Kobayashi et al., 2020). The AUC-ROC metric can implicitly consider these factors to better discover the correlation. (2) The proportion of different labels output by the model may be unbalanced. Using AUC-ROC can to some extent alleviate this problem and prevent the influence of class imbalance from disturbing our analysis.

Considering the residual mechanism that is common in Transformer models, the hidden state of each layer can be seen as the accumulation of the hidden states calculated separately by the previous layers. To measure the contribution of all layers up to the  $l$ th layer, we define the accumulated AUC-ROC score  $R_l$ :

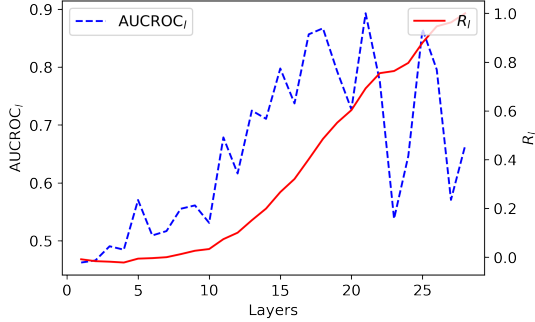
$$R_l = \frac{\sum_{i=1}^l (\text{AUCROC}_i - 0.5)}{\sum_{i=1}^N (\text{AUCROC}_i - 0.5)}. \quad (5)$$

Here, we quantify the positive contribution by calculating the difference between AUC-ROC and a baseline threshold of 0.5. The value of  $R_l$  represents the ratio of the contribution of the attention distributions on the label words of the target position in all layers up to the  $l$ -th layer.





(a) GPT2-XL (total 48 layers).



(b) GPT-J (total 28 layers).

Figure 3:  $AUCROC_l$  and  $R_l$  of each layer in GPT models. The result is averaged over SST-2, TREC, AGNews, and Emoc.  $AUCROC_l$  reaches 0.8 in deep layers, and  $R_l$  increases mainly in the middle and later layers.

### 2.3.2 Results and Analysis

Figure 3a and Figure 3b show the correlation metrics of each layer for GPT2-XL and GPT-J, respectively. The result is averaged over four datasets. Firstly, the  $AUCROC_l$  of the deep layers reaches a high score of 0.8, indicating a strong correlation between the attention distributions on the label words of the target position and the model’s final prediction. Secondly, the cumulative contributions  $R_l$  of the first few layers are near 0, while the score increases significantly in the middle and later layers. This phenomenon demonstrates that the classification decision of the model mainly takes place in the deep layers. From these two points, we validate that the model extracts the information from the positions of the label words to form the final prediction.

## 3 Applications Derived from Our Anchor-Based Understanding

With the insights drawn from the validated hypothesis, in this section, we propose applications to improve the effectiveness and inference efficiency. We introduce an anchor re-weighting method in

§ 3.1 to adaptive adjust the contribution of demonstration examples. In § 3.2, we explore a context compression technique that reduces original textual inputs to anchor hidden states for accelerating the ICL inference. Besides, using the anchor distances distribution, we also perform an analysis to better understand the errors ICL made in real-world scenarios (§ 3.3). These applications gain verify the proposed hypothesis, shedding light on new directions for future improvements of ICL.

### 3.1 Anchor Re-Weighting

In this part, we establish a connection between ICL and logistic regression based on the previous analysis. Inspired by such a connection, we further propose an approach for enhancing the accuracy of ICL by re-weighting the label anchors.

#### 3.1.1 Analogy Between ICL and Logistic Regression

By approximating the ICL model as a weighted combination of classifiers and leveraging the correlation between attention distributions and final predictions, we make an analogy of ICL to ICL the logistic regression. Specifically, we demonstrate that the attention mechanisms in ICL resemble the calculation principles of logistic regression, indicating a structural resemblance between the two frameworks.

In § 2.3, we show that the output category of the model is strongly correlated with the attention values ( $A(q, p_1), \dots, A(q, p_C)$ ) between the target position  $q$  and the label word positions  $p_1, \dots, p_C$  at deep layers. Considering the residual mechanism of the Transformer model, the final output can be viewed as the sum of the results from previous layers. Besides, the results of each layer can be viewed as the sum of each single attention head. We can approximate the outputs of the ICL  $f$  as:

$$f \approx \sum_{l=1}^L \sum_{h=1}^H \gamma_{lh} f_{lh}, \quad (6)$$

where  $f_{lh}$  represents the classifier approximation of the  $h$ th attention head in the  $l$ th layer, and  $\gamma_{lh}$  denotes the weight of the classifier.  $f_{lh}$  outputs a probability vector of each category for the input  $x$  as follows:

$$f_{lh}(x) \approx \left( A_l^h(q, p_1), \dots, A_l^h(q, p_C) \right). \quad (7)$$

The approximation  $f_{lh}$  may differ from the actual one by a coefficient, but it does not affect our subsequent discussions and conclusions.

According to the calculation formula of the attention mechanism, for the  $h$ th head of the  $l$ th layer, we have:

$$\begin{aligned} & \Pr_{f_{lh}}(Y = i | X = x) \\ &= A_l^h(q, p_i) \\ &= \frac{\exp(\mathbf{q}_q^h \mathbf{k}_{p_i}^{hT} / \sqrt{d})}{\sum_{j=1}^N \exp(\mathbf{q}_q^h \mathbf{k}_j^{hT} / \sqrt{d})}, \end{aligned} \quad (8)$$

where  $\mathbf{q}_q^h$  represents the query vector corresponding to the target position,  $\mathbf{k}_{p_i}^h$  represents the key vector corresponding to the label word, and  $d$  represents the dimension of the key vectors.

By defining  $\mathbf{q}_q^h / \sqrt{d} = \hat{\mathbf{x}}_{lh}$  and  $\mathbf{k}_{p_i} - \mathbf{k}_{p_C} = \beta_{lh}^i$  (where  $l$  corresponds to the layer number), we can infer that:

$$\log \frac{\Pr_{f_{lh}}(Y = i | X = x)}{\Pr_{f_{lh}}(Y = C | X = x)} = \beta_{lh}^{iT} \hat{\mathbf{x}}_{lh}. \quad (9)$$

This is similar to the logistic regression model, where

$$\log \frac{\Pr_f(Y = i | X = x_t)}{\Pr_f(Y = C | X = x)} = \beta_0^i + \beta^{iT} \mathbf{x}. \quad (10)$$

$\beta_0^i$  and  $\beta^{iT}$  are learnable parameters, and  $\mathbf{x}$  is the feature vector corresponding to the input.

Based on the preceding discussions, we have established an analogy between the ICL model and logistic regression, emphasizing their structural similarity. We approximate the ICL model as a combination of classifiers that employ attention distributions to generate predictions. Furthermore, we demonstrate that the computation of attention distributions exhibits similarities with the calculation principles of logistic regression. This correspondence implies that both frameworks operate on similar principles.

### 3.1.2 Anchor Re-Weighting Method

Inspired by the relation ICL and logistic regression, we add a learnable  $\beta_0^i$  to  $f_{lh}$  in Eq. (9):

$$\log \frac{\Pr_{f_{lh}}(Y = i | X = x)}{\Pr_{f_{lh}}(Y = C | X = x)} = \beta_0^i + \beta_{lh}^{iT} \hat{\mathbf{x}}_{lh}. \quad (11)$$

This is equivalent to adjust the weights of  $A_l^h(q, p_i)$ , which can be expressed as

$$\begin{aligned} f_{lh}(x) &\approx (\exp(\beta_{lh}^1) A_l^h(q, p_1), \\ &\quad \dots, \exp(\beta_{lh}^C) A_l^h(q, p_C)), \end{aligned} \quad (12)$$

where  $\beta_{lh}^1, \dots, \beta_{lh}^C$  are learnable parameters.

We manipulate the attention mechanism of the model to implement this re-weighting mechanism. Please refer to the details in Appendix F.

To train a reweighting vector  $\beta = \{\beta_{lh}^i\}$ , we use an additional training set  $(\mathbf{X}_{train}, \mathbf{Y}_{train})$ . On the training set, we concatenate normal examples to training data to perform ICL, and optimize  $\beta$  with respect to the classification loss function  $\mathcal{L}$ :

$$\beta = \arg \min_{\beta} \mathcal{L}(\mathbf{X}_{train}, \mathbf{Y}_{train}). \quad (13)$$

Metaphorically, this is equivalent to "re-weighting the anchors" in ICL. It can also be seen as an adjustment of the contribution of demonstration examples since their information has been aggregated into the anchors as suggested by our previous analysis.

### 3.1.3 Experiments

To verify the effect of re-weighting, we choose one sample per class as normal demonstrations, and choose 4 extra samples per class from the task training dataset to train  $\beta$ . Consistent with the setups in § 2.2, we use 5 random seeds and report the average result. For each random seed, we fix the demonstration and sample 1000 test samples from the test datasets. To optimize  $\beta$ , we use gradient descent with the Adam optimizer (Kingma and Ba, 2015) with a learning rate of 0.01,  $\beta_1 = 0.9$ ,  $\beta_2 = 0.999$ , and a batch size of 1 (due to memory constraint) for 10 epochs. Due to computational resource limitations, we cannot perform training on GPT-J, so we only adopt GPT2-XL for evaluation.

We compare re-weighting with two baselines: (1) Vanilla ICL with the same demonstration (1 shot per class) (2) Vanilla ICL with the training set of  $\beta$  added to the demonstrations (5-shot per class) for a fair comparison.

### 3.1.4 Results

As shown in Table 2, the proposed anchor re-weighting method significantly improves the performance of in-context learning. Particularly, the effect is remarkable on the SST-2 and EmoC datasets. Note that adding more demonstration examples for vanilla in-context learning may not bring a stable accuracy boost due to the potential noise introduced, as discussed in (Zhao et al., 2021). Different from vanilla ICL which utilizes the extra examples to form a demonstration, we train a re-weighting vector  $\beta$  to adjust the contribution of different label anchors. In this way, we reduce the length of the input context and thus bring (almost) no extra cost to the inference speed. The consistent improvements of our method suggest that the

re-weighting could be a better alternative to exploit the demonstration examples.

### 3.2 Anchor-Only Context Compression

We further explore a context compression technique that reduces original textual inputs to anchor hidden states for accelerating the ICL inference.

#### 3.2.1 Method

In § 2.3, we verify that the model’s output heavily relies on the label words, which collect information from demonstration examples during the forward propagation. We also notice that in auto-regressive language models such as GPT, the hidden state of each word depends only on the preceding words. In other words, the information aggregation process of label words is independent of the subsequent words. Therefore, we can compute the hidden states of the label words  $\mathbf{H} = \{\{h_l^i\}_{l=1}^N\}_{i=1}^C$  (where  $h_l^i$  represents the  $l$ -th layer’s hidden state of the  $i$ -th label word in the demonstration). We concatenate  $h_l^1, \dots, h_l^C$  in front of the input at each layer during inference. In this way, the model can perform inference without requiring the entire input, and thus the inference can be sped up.

In preliminary experiments, we find that the hidden states of the label words alone are not sufficient for the model to complete the ICL task. We speculate the reason is that the formatting information is also important for ICL to identify the output space on the target position. Therefore, we collect both the hidden states corresponding to the formatting and the hidden states corresponding to the label words and concatenate them together before inference, which we name as **Hidden<sub>anchor</sub>**.

#### 3.2.2 Experiments

We follow the same experimental settings as adopted in § 2.2. For comparison with **Text<sub>anchor</sub>**, we also implement two baselines for input compression (referred to as **Hidden<sub>anchor</sub>** in the text):

**Text<sub>anchor</sub>**: Concatenating the formatting text and target words before the text to be predicted, instead of concatenating them with the hidden states at each layer.

**Hidden<sub>random</sub>**: Randomly selecting the same number of words as in the Hidden method from the entire input text and concatenating their corresponding hidden states in front of the hidden states at each layer.

These two methods have the same efficiency as the **Hidden<sub>anchor</sub>** method. We evaluate the proposed

compression methods using the label loyalty and word loyalty introduced in § 2.2, as well as the original classification accuracy.

#### 3.2.3 Results

The results obtained on two models are shown in Table 3. The proposed compression method, **Hidden<sub>anchor</sub>**, achieves the best results among the three compression methods on all metrics and for both models. For example, with the GPT-J model, the compression method with anchor states only leads to a 1.5 accuracy drop compared to the uncompressed situation, indicating that the compression introduces negligible information loss. Further, we estimate the efficiency improvements over the original ICL. As shown in Table 4, the speed-up ratio ranges from  $1.1 \times$  to  $2.6 \times$ , as the efficiency gain is influenced by the total length of the demonstrations  $L_{\text{demo}}$  and the length of the text to be predicted  $L_x$ . We refer readers to Appendix G for a more elaborated analysis of the speed-up ratios. Besides, we observe that the acceleration effect is more pronounced in the GPT-J model compared to GPT2-XL, demonstrating its great potential to apply to larger language models.

### 3.3 Anchor Distances for Error Diagnosis

Lastly, we perform an error analysis for ICL by utilizing the relationships of the key vectors corresponding to the label words.

#### 3.3.1 Method

In § 2.3, we verify the correlation between the attention weights  $(A_l(q, p_1), \dots, A_l(q, p_C))$  and the model’s output results. Here,  $p_1, \dots, p_C$  denotes the label word position indexes, and  $q$  is the target position. For a single attention head, the attention score is computed as:

$$A_l^h(q, p_i) = \frac{\exp(\mathbf{q}_q \mathbf{k}_{p_i}^T / \sqrt{d})}{\sum_{j=1}^N \exp(\mathbf{q}_q \mathbf{k}_j^T / \sqrt{d})}. \quad (14)$$

This implies that  $A_l^h(q, p_i)$  is influenced by  $\mathbf{q}_q \mathbf{k}_{p_i}^T$ , i.e., the similarity between the key and query vectors. Therefore, if the key vectors  $\mathbf{k}$  of label words  $p_i$  and  $p_k$  are close,  $A_l^h(q, p_i)$  and  $A_l^h(q, p_k)$  will be relatively close for any input. Furthermore, considering the distribution of query vectors  $\mathbf{q}_q$ , we employ a PCA-like method to extract the components of the key vectors along the directions with significant variations in  $\mathbf{q}_q$ , and concatenate all heads to get feature  $\hat{\mathbf{k}}$  (see Appendix H for details).

Method	SST-2	TREC	AGNews	EmoC	Average
Vanilla In-context Learning ( 1-shot per class )	61.28	57.56	73.32	15.44	51.90
Vanilla In-context Learning ( 5-shot per class )	64.75	60.40	52.52	9.80	46.87
Anchor Re-weighting (1-shot per class)	<b>90.07</b>	<b>60.92</b>	<b>81.94</b>	<b>41.64</b>	<b>68.64</b>

Table 2: The effect after adding parameter  $\beta_0^i$ . For AGNews, due to the length limit, we only include three examples for each class as a demonstration. Our Anchor Re-weighting method achieves the best performance overall tasks.

Method	Label Loyalty	Word Loyalty	Acc.
ICL (GPT2-XL)	100.00	100.00	51.90
Text <sub>anchor</sub>	51.05	36.65	38.77
Hidden <sub>random</sub>	44.25	6.62	31.80
Hidden <sub>anchor</sub>	<b>79.47</b>	<b>62.17</b>	<b>45.04</b>
ICL (GPT-J)	100.00	100.00	56.82
Text <sub>anchor</sub>	53.45	43.85	40.83
Hidden <sub>random</sub>	47.84	1.12	39.72
Hidden <sub>anchor</sub>	<b>89.06</b>	<b>75.04</b>	<b>55.59</b>

Table 3: Results of different compression methods on GPT2-XL and GPT-J (averaged over SST-2, TREC, AGNews, and EmoC). Acc. denotes accuracy. The highest value excluding Vanilla ICL is marked in bold. Our method achieves the best performance among compression methods.

Model	SST-2	TREC	AGNews	EmoC
GPT2-XL	1.1×	2.5×	1.5×	1.4×
GPT-J	1.5×	2.6×	2.2×	1.9×

Table 4: Acceleration ratios after applying the Hidden<sub>random</sub> method on GPT2-XL and GPT-J.

The confusion between categories can then be measured by evaluating the distance between  $\hat{\mathbf{k}}$ :

$$\text{Confusion}_{ij}^{\text{pred}} = \frac{\|\hat{\mathbf{k}}_{\mathbf{p}_i} - \hat{\mathbf{k}}_{\mathbf{p}_j}\|}{\max_{s \neq t} \|\hat{\mathbf{k}}_{\mathbf{p}_s} - \hat{\mathbf{k}}_{\mathbf{p}_t}\|}, \quad (15)$$

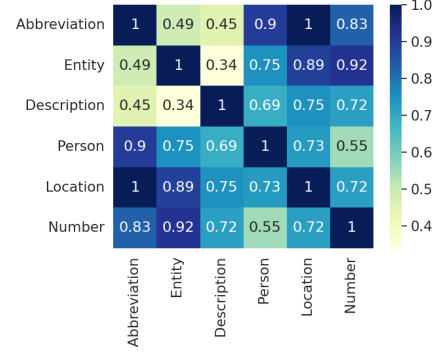
where  $\text{Confusion}_{ij}^{\text{pred}}$  is a value that does not exceed 1. A larger  $\text{Confusion}_{ij}^{\text{pred}}$  indicates a lighter degree of confusion between label categories.

### 3.3.2 Settings

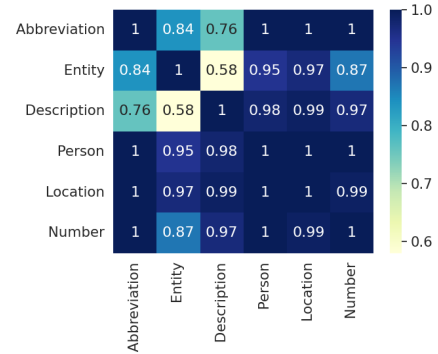
We select GPT2-XL and the TREC dataset, as we observe that the model exhibits significant confusion between certain categories while little confusion in others. Here we use the whole 500 samples of the TREC test set, and sample 1 demonstration per class for convenience of analysis.

### 3.3.3 Experiments

We measure the actual model confusion score  $\text{Confusion}_{ij}$  between category  $i$  and category  $k$  us-



(a) Confusion matrix of  $\text{Confusion}_{ij}^{\text{pred}}$ .



(b) Confusion matrix of  $\text{Confusion}_{ij}$ .

Figure 4: Predicted confusion matrix and real confusion matrix on TREC. We set the undefined to 1 diagonal for better visualization. Two heatmaps are similar for confusing category pairs, especially in light-color blocks.

ing the AUC-ROC metric (detailed in Appendix I). The heatmap with  $\text{Confusion}_{ij}^{\text{pred}}$  and  $\text{Confusion}_{ij}$  is plotted for comparison.

### 3.3.4 Results

As shown in Figure 4, the proposed approximation metric based on the anchor vectors can identify the most severe confusion case (Description-Entity) and performs reasonably well for relatively high confusion categories (Entity-Abbreviation, Description-Abbreviation). This high correlation indicates that ICL makes errors in categories with



similar label anchors. Overall, this result demonstrates that our anchor-based analysis framework could become an interpretable tool for better understanding the errors of ICL.

## 4 Related Work

The existing literature on in-context learning analysis can be broadly divided into two streams, each focusing on different aspects. The first stream explores the influencing factors of ICL based on input perturbation, such as the order (Min et al., 2022b), the formatting (Kim et al., 2022; Wei et al., 2022), and the selection of the demonstration (Liu et al., 2022). Designing proper demonstration construction strategies (Ye et al., 2023; Li et al., 2023) and calibration techniques (Zhao et al., 2021; Min et al., 2022a) could bring clear boosts to the ICL performance. The second stream investigates the inner working mechanism of ICL through different conceptual lenses, such as making an analogy of ICL to gradient descent (von Oswald et al., 2022; Dai et al., 2022) and viewing the process of ICL as a Bayesian inference (Xie et al., 2022).

In this paper, we provide a novel perspective by examining the information flow in language models to gain an understanding of ICL. Our approach offers new insights and demonstrates the potential for leveraging this understanding to improve the effectiveness, efficiency, and interpretability of ICL.

## 5 Conclusion

In this paper, we propose a hypothesis that label words serve as anchors in in-context learning for aggregating and distributing the task-relevant information flow. Experimental results with attention manipulation and analysis of predictions correlation consolidate the hypothesis holds well in GPT2-XL and GPT-J models. Inspired by the new understanding perspective, we propose three practical applications. First, an anchor re-weighting method is proposed to improve ICL accuracy. Second, we explore a demonstration compression technique to accelerate ICL inference. Lastly, we showcase an analysis framework to diagnose ICL errors on a real-world dataset. These promising applications again verify the hypothesis and open up new directions for future investigations on ICL.

## References

- Tom B. Brown, Benjamin Mann, Nick Ryder, Melanie Subbiah, Jared Kaplan, Prafulla Dhariwal, Arvind Neelakantan, Pranav Shyam, Girish Sastry, Amanda Askell, Sandhini Agarwal, Ariel Herbert-Voss, Gretchen Krueger, Tom Henighan, Rewon Child, Aditya Ramesh, Daniel M. Ziegler, Jeffrey Wu, Clemens Winter, Christopher Hesse, Mark Chen, Eric Sigler, Mateusz Litwin, Scott Gray, Benjamin Chess, Jack Clark, Christopher Berner, Sam McCandlish, Alec Radford, Ilya Sutskever, and Dario Amodei. 2020. Language models are few-shot learners. In *Advances in Neural Information Processing Systems 33: Annual Conference on Neural Information Processing Systems 2020, NeurIPS 2020, December 6-12, 2020, virtual*.
- Ankush Chatterjee, Kedhar Nath Narahari, Meghana Joshi, and Puneet Agrawal. 2019. [SemEval-2019 task 3: EmoContext contextual emotion detection in text](#). In *Proceedings of the 13th International Workshop on Semantic Evaluation*, pages 39–48.
- Damai Dai, Yutao Sun, Li Dong, Yaru Hao, Zhifang Sui, and Furu Wei. 2022. Why can gpt learn in-context? language models secretly perform gradient descent as meta optimizers. *ArXiv preprint*, abs/2212.10559.
- Qingxiu Dong, Lei Li, Damai Dai, Ce Zheng, Zhiyong Wu, Baobao Chang, Xu Sun, Jingjing Xu, and Zhifang Sui. 2023. A survey for in-context learning. *ArXiv preprint*, abs/2301.00234.
- Eduard Hovy, Laurie Gerber, Ulf Hermjakob, Chin-Yew Lin, and Deepak Ravichandran. 2001. Toward semantics-based answer pinpointing. In *Proceedings of the First International Conference on Human Language Technology Research*.
- Junyeob Kim, Hyuhng Joon Kim, Hyunsoo Cho, Hwiyeol Jo, Sang-Woo Lee, Sang goo Lee, Kang Min Yoo, and Taeuk Kim. 2022. Ground-truth labels matter: A deeper look into input-label demonstrations. *ArXiv*, abs/2205.12685.
- Diederik P. Kingma and Jimmy Ba. 2015. Adam: A method for stochastic optimization. In *3rd International Conference on Learning Representations, ICLR 2015, San Diego, CA, USA, May 7-9, 2015, Conference Track Proceedings*.
- Goro Kobayashi, Tatsuki Kuribayashi, Sho Yokoi, and Kentaro Inui. 2020. [Attention is not only a weight: Analyzing transformers with vector norms](#). In *Proceedings of the 2020 Conference on Empirical Methods in Natural Language Processing (EMNLP)*, pages 7057–7075.
- Xiaonan Li, Kai Lv, Hang Yan, Tianyang Lin, Wei Zhu, Yuan Ni, Guotong Xie, Xiaoling Wang, and Xipeng Qiu. 2023. [Unified demonstration retriever for in-context learning](#). *CoRR*, abs/2305.04320.
- Xin Li and Dan Roth. 2002. Learning question classifiers. In *COLING 2002: The 19th International Conference on Computational Linguistics*.

- Jiachang Liu, Dinghan Shen, Yizhe Zhang, Bill Dolan, Lawrence Carin, and Weizhu Chen. 2022. [What makes good in-context examples for GPT-3?](#) In *Proceedings of Deep Learning Inside Out (DeeLIO 2022): The 3rd Workshop on Knowledge Extraction and Integration for Deep Learning Architectures*, pages 100–114.
- Paul Michel, Omer Levy, and Graham Neubig. 2019. Are sixteen heads really better than one? In *Advances in Neural Information Processing Systems 32: Annual Conference on Neural Information Processing Systems 2019, NeurIPS 2019, December 8-14, 2019, Vancouver, BC, Canada*, pages 14014–14024.
- Sewon Min, Mike Lewis, Hannaneh Hajishirzi, and Luke Zettlemoyer. 2022a. [Noisy channel language model prompting for few-shot text classification](#). In *Proceedings of the 60th Annual Meeting of the Association for Computational Linguistics (Volume 1: Long Papers)*, pages 5316–5330.
- Sewon Min, Xinxin Lyu, Ari Holtzman, Mikel Artetxe, Mike Lewis, Hannaneh Hajishirzi, and Luke Zettlemoyer. 2022b. Rethinking the role of demonstrations: What makes in-context learning work? In *Conference on Empirical Methods in Natural Language Processing*.
- Catherine Olsson, Nelson Elhage, Neel Nanda, Nicholas Joseph, Nova DasSarma, Tom Henighan, Ben Mann, Amanda Askell, Yuntao Bai, Anna Chen, et al. 2022. In-context learning and induction heads. *ArXiv preprint*, abs/2209.11895.
- Alec Radford, Jeffrey Wu, Rewon Child, David Luan, Dario Amodei, Ilya Sutskever, et al. 2019. Language models are unsupervised multitask learners. *OpenAI blog*, 1(8):9.
- Karen Simonyan, Andrea Vedaldi, and Andrew Zisserman. 2013. Deep inside convolutional networks: Visualising image classification models and saliency maps. *CoRR*, abs/1312.6034.
- Richard Socher, Alex Perelygin, Jean Wu, Jason Chuang, Christopher D. Manning, Andrew Ng, and Christopher Potts. 2013. Recursive deep models for semantic compositionality over a sentiment treebank. In *Proceedings of the 2013 Conference on Empirical Methods in Natural Language Processing*, pages 1631–1642.
- Johannes von Oswald, Eyvind Niklasson, E. Randazzo, João Sacramento, Alexander Mordvintsev, Andrey Zhmoginov, and Max Vladymyrov. 2022. Transformers learn in-context by gradient descent. *ArXiv*, abs/2212.07677.
- Ben Wang and Aran Komatsuzaki. 2021. GPT-J-6B: A 6 Billion Parameter Autoregressive Language Model. <https://github.com/kingoflolz/mesh-transformer-jax>.
- Jason Wei, Xuezhi Wang, Dale Schuurmans, Maarten Bosma, Ed Huai hsin Chi, F. Xia, Quoc Le, and Denny Zhou. 2022. Chain of thought prompting elicits reasoning in large language models. *ArXiv*, abs/2201.11903.
- Sang Michael Xie, Aditi Raghunathan, Percy Liang, and Tengyu Ma. 2022. An explanation of in-context learning as implicit bayesian inference. In *The Tenth International Conference on Learning Representations, ICLR 2022, Virtual Event, April 25-29, 2022*.
- Jiacheng Ye, Zhiyong Wu, Jiangtao Feng, Tao Yu, and Lingpeng Kong. 2023. Compositional exemplars for in-context learning. *ArXiv preprint*, abs/2302.05698.
- Xiang Zhang, Junbo Jake Zhao, and Yann LeCun. 2015. Character-level convolutional networks for text classification. In *Advances in Neural Information Processing Systems 28: Annual Conference on Neural Information Processing Systems 2015, December 7-12, 2015, Montreal, Quebec, Canada*, pages 649–657.
- Zihao Zhao, Eric Wallace, Shi Feng, Dan Klein, and Sameer Singh. 2021. Calibrate before use: Improving few-shot performance of language models. In *Proceedings of the 38th International Conference on Machine Learning, ICML 2021, 18-24 July 2021, Virtual Event*, volume 139 of *Proceedings of Machine Learning Research*, pages 12697–12706.

## A Experimental Settings

For models, we use GPT2-XL (1.5B) (Radford et al., 2019) and GPT-J (6B) (Wang and Komatsuzaki, 2021) in this paper.

For datasets, we use a sentiment analysis task, Stanford Sentiment Treebank Binary (SST-2) (Socher et al., 2013), a question type classification task, Text REtrieval Conference Question Classification (TREC) (Li and Roth, 2002; Hovy et al., 2001), a topic classification task, AG’s news topic classification dataset (AGNews) (Zhang et al., 2015), a emotion classification task, EmoContext (EmoC) (Chatterjee et al., 2019). The ICL templates of these tasks are shown in Table 5.

## B Reason for Using Word Loyalty Besides Label Loyalty

Label loyalty alone may not capture changes in the probability of other words or the relative probability distribution of the label words. Word loyalty helps address this limitation, which is shown in Table 6.

## C Isolating Different Numbers of Layers

We study the impact of the numbers of isolated layers, as shown in Figures 5a and 5b. It can be

Table 5: Demonstration templates and label words, here  $\langle S1 \rangle$  represents the demonstration input,  $\langle S \rangle$  represents the input to be predicted, and  $\langle L \rangle$  represents the label word corresponding to the demonstration output. To save space, we only show one example for each task.

Task	Template	Label Words
SST-2	Review: $\langle S1 \rangle$ Sentiment: $\langle L \rangle$ Review: $\langle S \rangle$ Sentiment:	Positive, Negative
TREC	Question: $\langle S1 \rangle$ Answer Type: $\langle L \rangle$ Question: $\langle S \rangle$ Answer Type:	Abbreviation, Entity Description, Person Location, Number
AGNews	Article: $\langle S1 \rangle$ Answer: $\langle L \rangle$ Article: $\langle S \rangle$ Answer:	World, Sports Business, Technology
EmoC	Dialogue: $\langle S1 \rangle$ Emotion: $\langle L \rangle$ Dialogue: $\langle S \rangle$ Emotion:	Others, Happy Sad, Angry

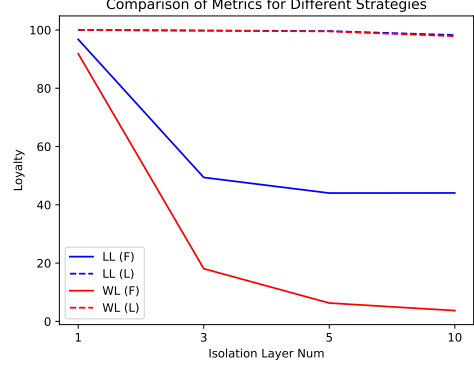
found that for the first layers, the more layers are isolated, the greater the impact on the model, while the increase in the number of isolated layers has a smaller impact on the model for the latter few layers. This further illustrates the important role of the information aggregation via label words in the shallow layers.

## D Results of Isolating Label Words on TREC and EmoC

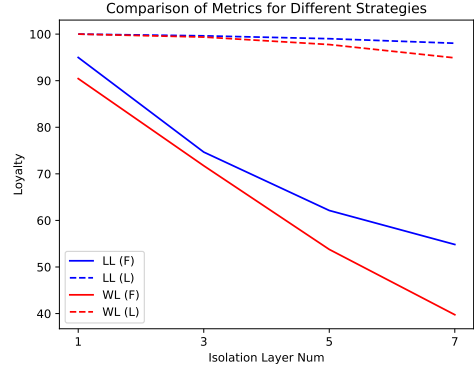
Relationship between the relative sizes of  $S_{wp}$ ,  $S_{pq}$ , and  $S_{ww}$  and the number of layers on TREC and EmoC are shown in Figure 6.

## E Details for the Calculation of AUCROC<sub>l</sub>

Suppose the positions of the label words in the input  $x$  are  $p_1, \dots, p_C$  (without loss of generality, we suppose  $p_i$  corresponds to the  $i$ th class), the targeted position is  $q$ , the sum of the attention matrices of each attention head at the  $l$  layer is  $A_l$ . We postulate that there’s a strong correlation between the attention distributions on the label words of the target position ( $A_l(q, p_1), \dots, A_l(q, p_C)$ ) and the model’s final prediction. We use the AUC-ROC score to quantify this correlation. We regard ( $A_l(q, p_1), \dots, A_l(q, p_C)$ ) as a classifier’s prediction for the model output label (that is,  $A_l(q, p_i)$  is equivalent to the probability of model output label  $i$ ), and compute the AUC-ROC value of this



(a) Effect of different numbers of isolated layers on GPT2-XL



(b) Effect of different numbers of isolated layers on GPT-J

Figure 5: Changes in Label Loyalty (LL) and Word Loyalty (WL) under different numbers of isolated layers. The letter F in brackets indicates the isolation of the label words in the first few layers, and L in brackets indicates the isolation of the label words in the last few layers. The loyalty of isolating the last layers is consistently high, while the loyalty of isolating the first layers decreases as the layer number increases.

prediction relative to the actual model output. We denote this as  $AUCROC_l$ .

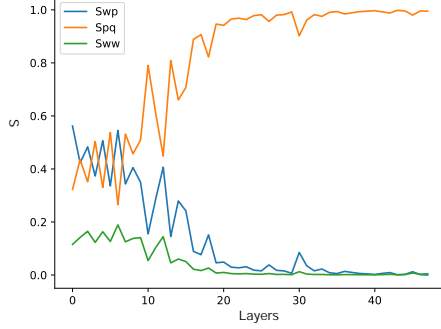
## F Implementation of Anchor Re-Weighting

To implement anchor re-weighting, in the specific computation process of the model, after calculating the attention matrix  $A_l^h$ , we multiply each  $A_l^h(q, p_i)$  by  $\exp(\beta_{lh}^i)$  and continue with the subsequent computations. In other words, for each attention head, we make the following modifications:

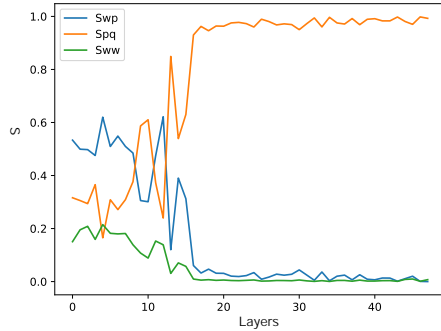
$$\begin{aligned}
 \text{Attention}_l^h(Q, K, V) &= \hat{A}_l^h V, \\
 A_l^h &= \text{softmax} \left( \frac{QK^T}{\sqrt{d}} \right), \\
 \hat{A}_l^h(k, j) &= \begin{cases} \exp(\beta_{lh}^i) A_l^h(k, j), & \text{if } k = q, j = p_i \\ A_l^h(k, j), & \text{otherwise} \end{cases}.
 \end{aligned} \tag{16}$$

Table 6: Results on a test sample with the label 'World' from AGNews.

Isolation Layer	Output Label	$V_5$ (sorted by probability)
First 5 layers	World	'n', 'The', 'Google', '<lendoftext>', 'A'
No isolation	World	'World', 'Technology', 'Politics', 'Israel', 'Human'



(a) Results on the TREC dataset



(b) Results on the EmoC dataset

Figure 6: Relationship between the relative sizes of  $S_{wp}$ ,  $S_{pq}$ , and  $S_{sw}$  and the number of layers on AGNews and EmoC.

## G The Factor of $L_{\text{demo}}$ and $L_x$

We discuss the factor of the total length of the demonstrations  $L_{\text{demo}}$  and the length of the text to be predicted  $L_x$  in compression. From Table 7, we can observe that the larger the ratio of total length to predicted text length, the more significant the efficiency improvement.

## H Calculation of $\hat{\mathbf{k}}$

For the sample sequence  $x_1, \dots, x_T$  to be predicted, we denote the query vectors of the target positions as  $\mathbf{q}_1, \dots, \mathbf{q}_T$ . We construct the matrix  $\hat{\mathbf{Q}} = (\mathbf{q}_1 - \bar{\mathbf{q}}, \dots, \mathbf{q}_T - \bar{\mathbf{q}})$  by subtracting the mean from the query vectors. Then, we sequentially find the  $M$  directions  $\mathbf{v}_1, \dots, \mathbf{v}_M$  with the  $M$  largest variation

	SST-2	TREC	AGNews	EmoC
GPT2-XL	$1.1 \times$	$2.5 \times$	$1.5 \times$	$1.4 \times$
GPT-J	$1.5 \times$	$2.6 \times$	$2.2 \times$	$1.9 \times$
$\frac{L_{\text{demo}} + L_x}{L_x}$	1.9	9.7	5.1	5.4

Table 7: Acceleration ratios after applying the Hidden<sub>anchor</sub> method and  $\frac{L_{\text{demo}} + L_x}{L_x}$

directions for the centralized  $\hat{\mathbf{q}}_1, \dots, \hat{\mathbf{q}}_T$ :

$$\begin{aligned}
 \mathbf{v}_1 &= \arg \max_{\|\mathbf{v}\|=1} \text{Var} \left\{ \mathbf{v}^\top \hat{\mathbf{Q}} \right\}, \\
 \mathbf{v}_2 &= \arg \max_{\|\mathbf{v}\|=1, \mathbf{v} \perp \mathbf{v}_1} \text{Var} \left\{ \mathbf{v}^\top \hat{\mathbf{Q}} \right\}, \\
 &\dots \\
 \mathbf{v}_M &= \arg \max_{\|\mathbf{v}\|=1, \mathbf{v} \perp \mathbf{v}_1, \dots, \mathbf{v} \perp \mathbf{v}_{M-1}} \text{Var} \left\{ \mathbf{v}^\top \hat{\mathbf{Q}} \right\}.
 \end{aligned} \tag{17}$$

Additionally, we denote the corresponding standard deviations  $\sqrt{\text{Var} \left\{ \mathbf{v}_i^\top \hat{\mathbf{Q}} \right\}}$  as  $\sigma_i$ .

We project the key vector  $\mathbf{k}$  onto the directions  $\mathbf{v}_1, \dots, \mathbf{v}_M$  and weight them by  $\sigma_1, \dots, \sigma_M$  to obtain the feature  $\hat{\mathbf{k}}$  that reflects the variation of the query vectors. ( $\hat{\mathbf{k}}_i = \sigma_i \mathbf{v}_i^\top \mathbf{k}$ )

We study the effect of  $M$  in the confusion matrix of Confusion <sub>$ij$</sub> <sup>pred</sup> (Figure 7). Since the result under various  $M$  is similar, we simply choose  $M = 10$  to calculate Confusion <sub>$ij$</sub> <sup>pred</sup>.

## I Calculation of Confusion <sub>$ij$</sub>

To measure the actual confusion between category  $i$  and category  $k$  for the model, we propose the metric Confusion <sub>$ij$</sub> :

We extract all test samples  $x_t$  with true labels  $i$  or  $k$ , as well as the probabilities  $p_i^t$  and  $p_j^t$  output by the model for categories  $i$  and  $k$  on these samples, respectively (normalized to sum up to 1). In other words, we obtain a classifier  $f$  that outputs the probabilities  $p_i^t$  and  $p_j^t$  for categories  $i$  and  $k$ , respectively, on the test samples  $x_t$ . We calculate the AUC-ROC value of this classifier  $f$  to obtain the degree of confusion between category  $i$  and  $k$ , denoted as Confusion <sub>$ij$</sub> . The calculated Confusion <sub>$ij$</sub>  is a value that does not exceed 1. The



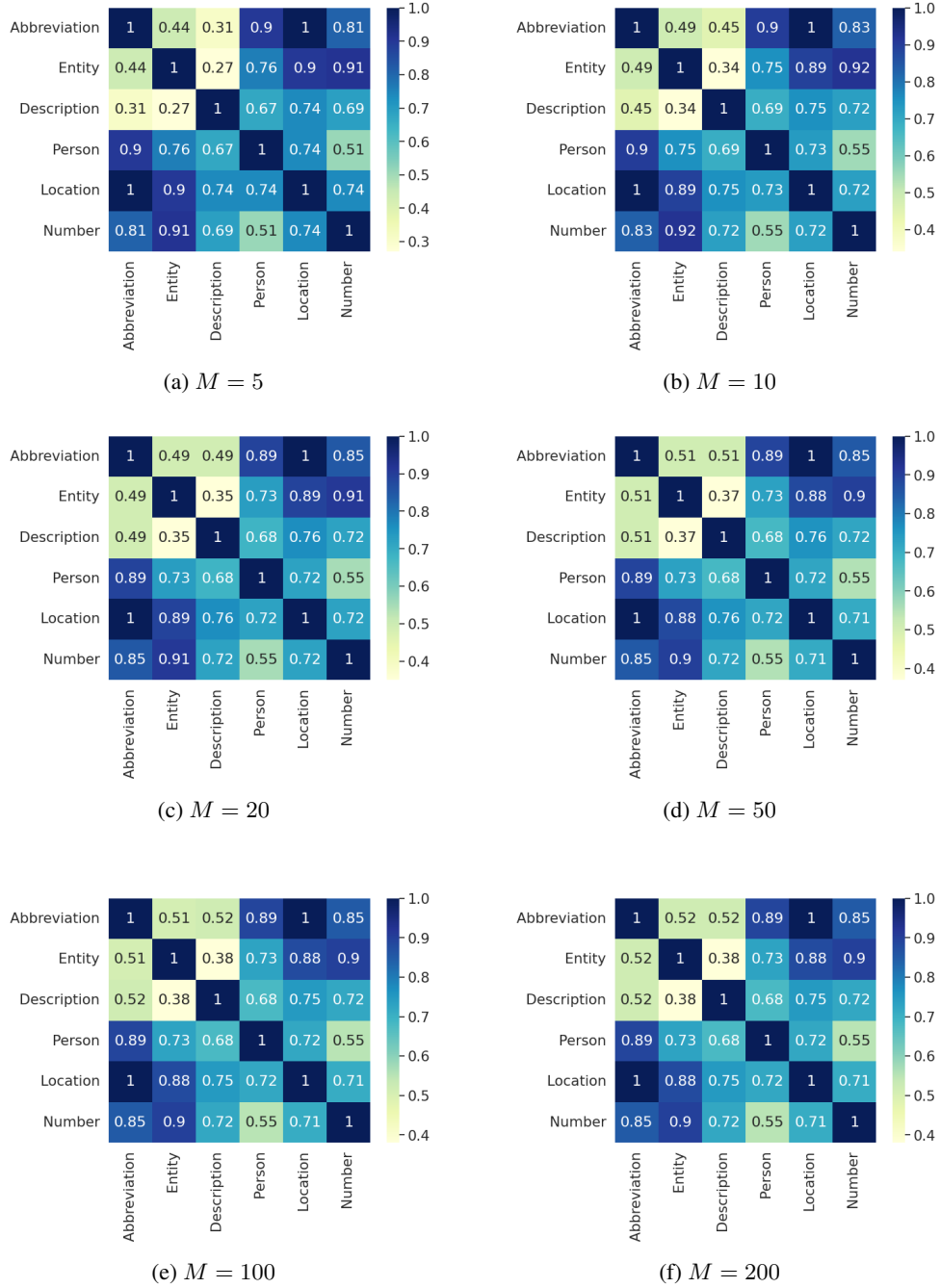


Figure 7: Predicted confusion matrixes under  $M = 5, 10, 20, 50, 100, 200$ .

closer  $\text{Confusion}_{ij}$  is to 1, the lighter the degree of confusion, and vice versa.

We use the above metric instead of directly analyzing the output labels of the model because previous work has indicated the issue of insufficient output probability calibration in ICL (Zhao et al., 2021), which is greatly affected by factors such as sample ordering and model preferences for label words. By using the defined degree of confusion  $\text{Confusion}_{ij}$ , we can implicitly mitigate the inter-

ference of insufficient probability calibration on the output labels, to some extent, obtain the degree of confusion of the model for different categories that better reflects the real situation, and reduce the interference of randomness.